Damping of Geodesic Acoustic Mode by Trapped Electrons

ZHANG Shuangxi (张双喜)[1,2], GAO Zhe (高喆)[3], WU Wentao (武文韬)[1], QIU Zhiyong (仇志勇)[4]

[1]Department of Modern Physics, University of Science and Technology of China, Hefei 230026, China
[2]Key Laboratory of Pulsed Power, Institute of Fluid Physics, China Academy of Engineering Physics, Mianyang 621900, China
[3]Department of Engineering Physics, Tsinghua University, Beijing 100084, China
[4]Institute for Fusion Theory and Simulation, Zhejiang University, Hangzhou 310027, China

Abstract We study the Landau resonance between geodesic acoustic mode (GAM) and trapped electrons as a GAM's collisionless damping. The assumption of $\bar{\omega}_{\rm de} \ll \omega_{\rm be}$ is adopted. The damping rate induced by trapped electrons is found to be an increasing function of q. In low q range, circulating-ion-induced damping rate is larger than that induced by trapped electrons. As q increases, the latter becomes larger than the former. The reason is that trapped electrons' resonant velocity is close to $v_{\rm te}$ from the lower side, whiles circulating ions' resonant velocity gets bigger further from $v_{\rm ti}$. So the number of resonant trapped electrons increases, whiles the number of resonant circulating ions decreases. The amplitude of damping rate induced by trapped electrons in the edge plasma can be comparable to that induced by circulating ions in the low q range. Another phenomenon we found is that in the chosen range of ϵ, the damping caused by trapped electrons has a maximum value at point ϵ_q for different q. The reason is that as ϵ is close to ϵ_q, trapped electorns' resonant velocity is close to $v_{\rm te}$.

Keywords: geodesic acoustic mode, landau resonance, trapped electrons, bounce frequency

PACS: *52.35.Py, 52.57.Fg, 52.38.Mf*

DOI: 10.1088/1009-0630/16/7/04

(Some figures may appear in colour only in the online journal)

1 Introduction

Geodesic acoustic modes (GAM) [1], is an electrostatic mode unique in toroidal confinement devices with geodesic curvature. The electrostatic potential of GAM is characterized by a toroidal mode number $n = 0$ and a poloidal mode number $m = 0$, and an $n = 0$ and $m = 1$ up-down anti-symmetric density perturbation [2−4]. GAM is extensively studied in the past decade due to its potential role in regulating the drift wave turbulences, which are generally believed to be one of the major candidate of anomalous transport in magnetic confinement fusion [5−7]. The excitation threshold and saturation level of GAM are determined by its damping mechanisms. In this paper we study the collisionless damping of GAM due to trapped electrons.

GAM, unlike its low frequency counterpart, has a finite collisionless damping. The collisionless damping of GAM due to resonant circulating ions has been intensively studied, while trapped ion effect on GAM is ignored since one typically has $\omega_{\rm G} \gg \omega_{\rm b,i}$. Here, $\omega_{\rm G}$ and $\omega_{\rm b,i}$ are respectively the GAM frequency and bounce frequency of trapped ions. The frequency of GAM, in the $T_{\rm e} \ll T_{\rm i}$ limit, is given by Ref. [8] $\omega_{\rm G}^2 = 7v_{\rm ti}^2(1 + 46/49q^2)/4R^2$, where $v_{\rm ti}$ is ions and electrons' thermal velocity respectively, q is the safety factor, and R is major radius. The effect of electrons on GAM collisionless damping, was believed to be small, since the characteristic frequency of electrons, i.e., the transit frequency of circulating electrons is too high for effective resonant energy exchange with GAM. However, large scale particle in cell simulation with kinetic electrons [9], shows that, the contribution of trapped electrons to GAM collisionless damping, can be comparable, or even larger than that due to ions. Furthermore, the experiments conducted in HL-2A [6] show that GAM's amplitude reduces with increasing electron cyclotron resonance heating (ECRH) power. One possible explanation is that with the heating of electron perpendicular energy by ECRH, more trapped electrons are formed, leading to enhanced GAM damping. As a matter of fact, the bounce frequency of deeply trapped electrons, $\omega_{\rm b} \approx \sqrt{\epsilon\mu B_0}/qR\sqrt{m}$ is comparable to $\omega_{\rm G}$ in the high q range in the edge plasma in tokamak, where the circulating ion resonance, which is usually the most effective wave particle resonance for GAM, is minimized. Here, ϵ is aspect ratio and μ is the magnetic moment. So it is expected that trapped electron

Landau damping is dominant in the high q regime of a collisionless plasma. Based on these considerations, we are motivated to study trapped electrons' effect on GAM's damping theoretically in this paper using drift kinetic theory assuming $k\rho_{\mathrm{i,e}} \ll 1$. Here, k is GAM's radial wavenumber and $\rho_{\mathrm{i,e}}$ is Larmor radius [10] for ions and electrons respectively. We will focus on the contribution from deeply trapped electrons for analytical progress, despite the fact that, more important roles may be played by barely trapped electrons [9].

The arrangement of this paper is as follows. In section 2, the calculation of perturbed density of ions and trapped electrons is carried out. In section 3, GAM's eigenfrequency and trapped-electron-induced damping are obtained. In section 4, some numerical examples are given to study reliability of GAM's eigenvalue and trapped electrons damping rate on parameters of magnetic field and plasma. Section 5 is the summary.

2 Perturbed density of circulating ions

In this paper, we adopt the magnetic field $\mathbf{B} = B_0[\mathbf{e}_\xi/(1+\epsilon\cos\theta) + \mathbf{e}_\theta\epsilon/q]$, which is of large aspect ratio and circular cross section. Here B_0 is the amplitude of equilibrium magnetic field, $\epsilon = r/R$ is assumed to be small but finite, ξ, θ are toroidal and poloidal unit vector respectively, and q is safety factor. If GAM's electrostatic potential can be decomposed as $\phi = \sum_{\omega,k} \tilde{\phi}_k(\theta)\exp[\mathrm{i}k(r-r_0) - \mathrm{i}\omega t]$, the k component of the response of particles can be described as $\tilde{f}_{q_1,k} = -q_1 F_{0q_1}\tilde{\phi}_k/T_{q_1} + \tilde{h}_{q_1,k}$, where $\tilde{\phi}_0$ is the poloidally-averaged zonal potential, q_1 is the particle's charge and $\tilde{h}$ is the non-adiabatic perturbed distribution, which satisfies the following drift kinetic equation [11,12]

$$\left(\omega - \omega_{\mathrm{d}q_1}\sin\theta + \mathrm{i}\omega_{\mathrm{t}q_1}\frac{\partial}{\partial\theta}\right)\tilde{h}_{q_1,k} = \frac{q_1 F_{0q_1}}{T_{q_1}}\omega\tilde{\phi}_{\mathrm{k}}, \quad (1)$$

where $\omega_{\mathrm{d}q_1} = \frac{v_\perp^2/2+v_\parallel^2}{2\omega_{q_1}R}k, \omega_{\mathrm{t}q_1} = v_\parallel/qR$.

2.1 Perturbed density of circulating ions

The trapped ion effect on GAM' damping is ignored due to $\omega_{\mathrm{G}} \gg \omega_{\mathrm{bi}}$. The solution of circulating ions concerned with Eq. (1) is given in Ref. [8]. The total perturbed distribution function is the summation of analytical solution of Eq. (1) and the adiabatic part

$$\tilde{f}_{\mathrm{i},k} = -\frac{eF_{0\mathrm{i}}}{T_{\mathrm{i}}}\sum_{l=-\infty}^{\infty}\tilde{\phi}_{k,l}\mathrm{e}^{\mathrm{i}l\theta} \times\left[1 - \sum_{m,n=-\infty}^{\infty}\mathrm{i}^{m-n}e^{\mathrm{i}(m-n)\theta}\frac{\omega J_m J_n}{\omega + (n-l)\omega_{\mathrm{ti}}}\right], \quad (2)$$

where J_m, J_n are bessel functions of $\omega_{\mathrm{di}}/\omega_{\mathrm{ti}}$ and $F_{0\mathrm{i}}$ is Maxwellian distribution. In our paper, modes of $m = 0, \pm1$ are kept due to the ordering relationship $\tilde{\phi}_{k,m}/\tilde{\phi}_{k,0} \sim (\omega_{\mathrm{di}}/\omega_{\mathrm{ti}})^m$ given in Refs. [13,14] because of $\omega_{\mathrm{di}}/\omega_{\mathrm{ti}} \ll 1$. The perturbed densities of $m = 0, \pm1$ are obtained by integrating Eq. (2) in velocity space

$$\tilde{n}_{\mathrm{i},k,0} = -\frac{en_{k,0}k^2q^2v_{\mathrm{ti}}^2\tilde{\phi}_{k,0}}{2\omega_{\mathrm{i}}^2T_{\mathrm{i}}}\left(\frac{Z(\zeta_{\mathrm{i}})}{2\zeta_{\mathrm{i}}} + \frac{Z_1(\zeta_{\mathrm{i}})}{2} + Z_3(\zeta_{\mathrm{i}})\right) + \frac{\mathrm{i}en_{k,0}\omega kq^2R\tilde{\phi}_{k,1}}{\omega_{\mathrm{i}}T_{\mathrm{i}}}\left(\frac{Z(\zeta_{\mathrm{i}})}{2\zeta_{\mathrm{i}}} + Z_1(\zeta_{\mathrm{i}})\right), \quad (3)$$

$$\tilde{n}_{\mathrm{i},k,\pm1} = \frac{-en_0\tilde{\phi}_{k,\pm1}}{T_{\mathrm{i}}}(1+\zeta_{\mathrm{i}}Z(\zeta_{\mathrm{i}})) \times\frac{\mathrm{i}en_0\tilde{\phi}_{k,0}k\omega q^2R}{2\omega_{\mathrm{i}}T_{\mathrm{i}}}\left(\frac{Z(\zeta_{\mathrm{i}})}{2\zeta_{\mathrm{i}}} + Z_1(\zeta_{\mathrm{i}})\right), \quad (4)$$

where $\zeta_{\mathrm{i}} = \omega qR/v_{\mathrm{ti}}$. To get the above equations, the following integral formulas are used.

$$Z(\zeta) = \frac{1}{\sqrt{\pi}}\int\frac{\exp\left(-v_\parallel^2\right)}{v_\parallel - \zeta}\mathrm{d}v_\parallel, \quad (5)$$

$$Z_1(\zeta) = \frac{1}{\sqrt{\pi}}\int\frac{\exp\left(-v_\parallel^2\right)v_\parallel^2}{v_\parallel^2 - \zeta^2}\mathrm{d}v_\parallel = 1 + \zeta Z(\zeta), \quad (6)$$

$$Z_2(\zeta) = \frac{1}{\pi^{3/2}}\int 2\pi v_\perp\mathrm{d}v_\perp\mathrm{d}v_\parallel \times\frac{\exp\left(-v_\parallel^2 - v_\perp^2\right)\left(v_\parallel^2 + v_\perp^2/2\right)}{v_\parallel^2 - \zeta^2} = \frac{Z(\zeta)}{2\zeta} + Z_1(\zeta), \quad (7)$$

$$Z_3(\zeta) = \frac{1}{\pi^{3/2}}\int 2\pi v_\perp\mathrm{d}v_\perp\mathrm{d}v_\parallel \times\frac{\exp\left(-v_\parallel^2 - v_\perp^2\right)\left(v_\parallel^2 + v_\perp^2/2\right)v_\parallel^2}{v_\parallel^2 - \zeta^2} = 1 + \zeta^2 Z_2(\zeta), \quad (8)$$

$$Z_4(\zeta) = \frac{1}{\pi^{3/2}}\int 2\pi v_\perp\mathrm{d}v_\perp\mathrm{d}v_\parallel \times\frac{\exp\left(-v_\parallel^2 - v_\perp^2\right)\left(v_\parallel^2 + v_\perp^2/2\right)^2}{v_\parallel^2 - \zeta^2} = \frac{Z(\zeta)}{2\zeta} + \frac{Z_1(\zeta)}{2} + Z_3(\zeta). \quad (9)$$

2.2 Perturbed density for trapped electrons

In toroidal devices such as tokamak, equilibrium magnetic field forms a magnetic mirror due to its magnetic field gradient. Part of electrons could be trapped by such magnetic mirror and bounce between the two mirror points. Trapped electrons' perturbed distribution is obtained by adopting the method used in Refs. [15-17], which transforms gyrokinetic orbit reference frame into banana orbit center reference frame to study the resonance between trapped particles' precessional frequency and Alfven wave's frequency. The poloidal angle of trapped electrons' bounce motion is

defined as θ. In this paper, only deeply trapped electrons are considered so that θ can be approximated as $\theta = \theta_{\rm b}\sin\eta$, where $\theta_{\rm b}$ is poloidal angle at the mirror point and η is ballooning angle centering on banana orbit center.

The trapped electrons' perturbed distribution function can be decomposed as $\tilde{f}_{{\rm e},k} = eF_0\tilde{\phi}_k/T_{\rm e} + \tilde{h}_k$. Non-adiabatic perturbed distribution $\tilde{h}_k$ transformed from gyro orbit center into banana orbit center is

$$\tilde{h}_{{\rm b},k} = \left(\sum\nolimits_h (-{\rm i})^h J_{\rm h}(\lambda_{\rm b})\,{\rm e}^{{\rm i}\eta h}\right)\tilde{h}_{{\rm e},k}, \tag{10}$$

where $\lambda_{\rm b} = \theta_{\rm b}(\bar{\omega}_{\rm de}/\omega_{\rm b})$, $\bar{\omega}_{\rm de} = kv_{\rm te}^2/R\omega_{\rm ce}$, and $\omega_{\rm ce} = -eB/m_{\rm e}$. For small banana width, $\lambda_{\rm b} \ll 1$ which ensures $J_0(\lambda_{\rm b}) \approx 1$ and $J_h(\lambda_{\rm b}) \ll 1$. Thus at the lowest and relevant order, Eq. (10) gives $\tilde{h}_{{\rm b},k} = \tilde{h}_k$. For deeply trapped electrons, the bounce frequency is approximated as $\omega_{\rm be} = \epsilon^{1/2}v/qR$ and $v_\parallel\partial/qR\partial\theta = \omega_{\rm b}\partial/\partial\eta$. Eq. (1) is reformulated for trapped electrons' $\tilde{h}_{{\rm b},k}$ [15,18]

$$\left(\omega - \bar{\omega}_{\rm de}\sin\theta + {\rm i}\frac{\partial}{\partial\eta}\right)\tilde{h}_k = \frac{-eF_{0{\rm i}}}{T_{\rm e}}\omega\left(\sum\nolimits_h {\rm i}^h J_h(\lambda_{\rm b})\,{\rm e}^{-{\rm i}\eta h}\right)\tilde{\phi}_k. \tag{11}$$

To solve Eq. (11), only terms of $h = 0$ are kept in the right side of Eq. (11) due to $\tilde{\lambda} \ll 1$. And $\tilde{\phi}_k$ is approximated as

$$\tilde{\phi}_k = \tilde{\phi}_{k,0} + \tilde{\phi}_{k,1}{\rm e}^{{\rm i}\theta} + \tilde{\phi}_{k,-1}{\rm e}^{-{\rm i}\theta}. \tag{12}$$

${\rm e}^{\pm{\rm i}\theta}$ in ϕ_k in Eq. (12) are expanded by the Bessel series of η and only terms of $|n| \le 1$ are kept because of $\theta = \theta_{\rm b}\sin\eta$ and $\theta_{\rm b} \ll 1$. Noticing the following equities $\theta = \theta_{\rm b}\sin\eta, \sin\eta = \cos(\pi/2-\eta), {\rm e}^{{\rm i}z\cos\eta} = \sum_{-\infty}^{+\infty}{\rm i}^n J_n(z)\,{\rm e}^{{\rm i}n\eta}$, and ignoring Bessel functions of $n > 1$ in ${\rm e}^{{\rm i}z\cos\eta}$, ${\rm e}^{\pm{\rm i}\theta}$ are expanded as

$$\exp(\pm{\rm i}\theta) = J_0(\pm\theta_{\rm b}) - J_1(\pm\theta_{\rm b})\left({\rm e}^{-{\rm i}\eta} - {\rm e}^{{\rm i}\eta}\right). \tag{13}$$

Substituting Eq. (13) into Eq. (12) gives

$$\tilde{\phi}_k = \widetilde{\phi}_{k,0} + \tilde{\phi}_{k,1}J_0(\theta_{\rm b}) + \tilde{\phi}_{k,-1}J_0(-\theta_{\rm b}) - \left(\tilde{\phi}_{k,1}J_1(\theta_{\rm b}) - \tilde{\phi}_{k,-1}J_1(\theta_{\rm b})\right)\left({\rm e}^{-{\rm i}\eta} - {\rm e}^{{\rm i}\eta}\right). \tag{14}$$

The perturbed distribution functions of $m = 0, \pm1$ are obtained by substituting Eq. (14) into Eq. (11).

In this paper, $|\bar{\omega}_{\rm de}| = |\bar{\omega}_{\rm di}|$ is ensured by the assumption of temperature equilibrium between ions and electrons. Besides that, $k\rho_{\rm i} \approx 1$ suggested by experiments [4] leads to $|\bar{\omega}_{\rm de}| \approx v_{\rm ti}/10R$. Thus $|\bar{\omega}_{\rm de}|/\omega_{\rm G} \ll 0.1$ holds concerned with GAM's frequency given in Ref. [8]. So it's plausible to adopt the ordering relationship $\bar{\omega}_{\rm de}/\omega \sim \bar{\omega}_{\rm de}/\omega_{\rm be} \ll 1$ when solving Eq. (11) and keep it's solution up to order $O(\frac{\bar{\omega}_{\rm de}}{\omega})$.

The perturbed distribution responding to perturbed electrostatic potential of $m = 0$ in banana orbit center frame is derived by iteratively solving drift kinetic equations up to first order $O(\frac{\bar{\omega}_{\rm de}}{\omega})$. The iterative equations are

$$\left(\omega + {\rm i}\omega_{\rm b}\frac{\partial}{\partial\eta}\right)g_{k,1} = \frac{-eF_{0{\rm e}}}{T_{\rm e}}\omega\left(\widetilde{\phi}_{k,0} + \tilde{\phi}_{k,1}J_0(\theta_{\rm b}) + \tilde{\phi}_{k,-1}J_0(-\theta_{\rm b})\right), \tag{15}$$

$$\left(\omega + {\rm i}\omega_{\rm b}\frac{\partial}{\partial\eta}\right)g_{k,2} = \frac{\theta_{\rm b}\bar{\omega}_{\rm de}g_{k,1}}{2{\rm i}}\left({\rm e}^{{\rm i}\eta} - {\rm e}^{-{\rm i}\eta}\right). \tag{16}$$

Approximation $\sin\theta \approx \theta = \theta_{\rm b}\sin\eta$ is used in the right hand of Eq. (16). The solutions of Eq. (15) and Eq. (16) are

$$\tilde{g}_{k,1} = \frac{-eF_{0{\rm e}}}{T_{\rm e}}\left[\tilde{\phi}_{{\rm b},k,0} + \tilde{\phi}_{{\rm b},k,1}J_0(\theta_{\rm b}) + \tilde{\phi}_{{\rm b},k,-1}J_0(-\theta_{\rm b})\right], \tag{17}$$

$$\tilde{g}_{k,2} = -\frac{eF_{0{\rm e}}}{T_{\rm e}}\frac{\bar{\omega}_{\rm de}}{2{\rm i}}\left[\tilde{\phi}_{k,0} + \tilde{\phi}_{k,1}(\theta_{\rm b})J_0(\theta_{\rm b}) + \tilde{\phi}_{k,-1}J_0(-\theta_{\rm b})\right] \times\left(\frac{2\omega_{\rm b}\theta_{\rm b}\cos\eta}{\omega^2-\omega_{\rm b}^2} + \frac{{\rm i}2\omega\theta_{\rm b}\sin\eta}{\omega^2-\omega_{\rm b}^2}\right). \tag{18}$$

The perturbed distribution functions responding to perturbed electrostatic potential of $m = \pm1$ in banana orbit center frame are derived by solving the following drift kinetic equation

$$\left(\omega - \bar{\omega}_{\rm de}\sin\theta + {\rm i}\omega_{\rm b}\frac{\partial}{\partial\eta}\right)\tilde{g}_{k,3} = \frac{eF_{\rm e}}{2T_{\rm e}}\omega\theta_{\rm b}\left(\tilde{\phi}_{k,1} - \tilde{\phi}_{k,-1}\right)\left({\rm e}^{-{\rm i}\eta} - {\rm e}^{{\rm i}\eta}\right). \tag{19}$$

Here, approximation $J_1(\theta_{\rm b}) = \theta_{\rm b}/2$ is used. By noting $\tilde{\phi}_{k,\pm1}/\tilde{\phi}_{k,0} \sim |\omega_{\rm de}|/\omega$, and keeping terms to the same order as $\tilde{g}_{k,2}$, the solution of Eq. (19) becomes

$$\tilde{g}_{k,3} = \frac{-eF_{0{\rm e}}\omega\left(\tilde{\phi}_{k,1} - \tilde{\phi}_{k,-1}\right)}{T_{\rm e}}\times\left(\frac{2\theta_{\rm b}\omega_{\rm b}\cos\eta}{\omega^2-\omega_{\rm b}^2} + \frac{{\rm i}2\omega\theta_{\rm b}\sin\eta}{\omega^2-\omega_{\rm b}^2}\right). \tag{20}$$

The terms containing $\omega_{\rm be}$ in the numerator of perturbed distribution will vanish due to trapped particles moving in two opposite bounce directions along the magnetic field line as that circulating particles do [15–17]. Combining Eqs. (17),(18),(20), the non-adiabatic distribution functions of $m = 0, \pm1$ are obtained as

$$\tilde{h}_{k,0} = \frac{-eF_{0{\rm e}}}{T_{\rm e}}\left(\tilde{\phi}_{k,0} + \tilde{\phi}_{k,1} + \tilde{\phi}_{k,-1}\right), \tag{21}$$

$$\tilde{h}_{k,\pm1} = \mp\frac{eF_{0{\rm e}}}{T_{\rm e}}\frac{\bar{\omega}_{\rm de}\omega}{2{\rm i}}\frac{{\rm e}^{\pm{\rm i}\theta}}{\omega^2-\omega_{\rm b}^2}\left(\tilde{\phi}_{k,0} + \tilde{\phi}_{k,1} + \tilde{\phi}_{k,-1}\right) \mp\frac{eF_{0{\rm e}}\omega^2}{T_{\rm e}}\frac{{\rm e}^{\pm{\rm i}\theta}}{\omega^2-\omega_{\rm b}^2}\left(\tilde{\phi}_{k,1} - \tilde{\phi}_{k,-1}\right). \tag{22}$$

The perturbed densities are obtained by integrating the above equations in velocity space. For trapped particles, the integration in the velocity space can be written as

$$\langle(\cdots)\rangle = 2\pi \sum_{\sigma=\pm1} \int_0^{\infty} \mathrm{d}\varepsilon \int_{\varepsilon/B_{\max}}^{\varepsilon/B} \frac{B}{|v_{\parallel}|}(\cdots)\mathrm{d}\mu, \quad (23)$$

with $B_{\max} = B_0(1+\epsilon)$ and $B_{\min} = B_0(1-\epsilon)$ which are experienced by trapped electrons, and ε, μ are trapped particles' kinetic energy and magnetic moment respectively with the normalized mass. Since Eq. (22) does not explicitly depend on θ_{b}, for deeply trapped particles, we can approximately write Eq. (23) as Ref. [15]

$$\begin{aligned}\langle(\cdots)\rangle &\approx 8\pi\epsilon^{1/2}\int_0^{\infty}\varepsilon^{1/2}\mathrm{d}\varepsilon\cos(\theta/2)(\cdots)\\ &\approx 4\sqrt{2}\pi\epsilon^{1/2}\int_0^{\infty}\mathrm{d}v v^2(\cdots). \end{aligned} \quad (24)$$

Based on Eq. (22), the non-adiabatic perturbed density components of $m = \pm1$ are carried out by integrating $\tilde{h}_{k,s}$ in trapped particles' velocity space through the following integral formula,

$$\begin{aligned}\int_0^{+\infty}\mathrm{d}v\frac{v^2F_0}{\omega_{\mathrm{b}}^2-\omega^2} &= \frac{q^2R^2}{\epsilon\pi^{3/2}v_{\mathrm{te}}^2}\int_0^{+\infty}\mathrm{d}v\frac{v^2\mathrm{e}^{-v^2}}{v^2-\zeta_{\mathrm{e}}^2}\\ &= \frac{q^2R^2}{2\epsilon\pi v_{\mathrm{te}}^2}\left(1+\zeta_{\mathrm{e}}Z(\zeta_{\mathrm{e}})\right), \end{aligned} \quad (25)$$

where $\zeta_{\mathrm{e}} = \omega qR/\sqrt{\epsilon}v_{\mathrm{te}}$, $F_{0\mathrm{e}} = \exp\left(-v^2/v_{\mathrm{e}}^2\right)/\pi^{3/2}v_{\mathrm{te}}^3$, and v_{te} is electrons' thermal velocity. Eq. (6) is used to get the last equality in Eq. (25). The total perturbed densities of $m = \pm1$ shown below are obtained by combining the non-adiabatic and adiabatic perturbed densities

$$\tilde{n}_{\mathrm{et},k,0} = \frac{-\sqrt{2\epsilon}en_0}{T_{\mathrm{e}}}\left(\tilde{\phi}_{k,1}+\tilde{\phi}_{k,-1}\right), \quad (26)$$

$$\begin{aligned}\tilde{n}_{\mathrm{et},k,\pm1} &= \frac{\sqrt{2\epsilon}en_0\tilde{\phi}_{k,\pm1}}{T_{\mathrm{e}}} \pm \frac{en_0 2\sqrt{2}q^2R^2}{\pi^{1/2}\sqrt{\epsilon}T_{\mathrm{e}}}\frac{(1+\zeta_{\mathrm{e}}Z(\zeta_{\mathrm{e}}))}{v_{\mathrm{te}}^2}\\ &\times\left[\frac{\bar{\omega}_{\mathrm{de}}\omega}{2\mathrm{i}}\left(\tilde{\phi}_{k,0}+\tilde{\phi}_{k,1}+\tilde{\phi}_{k,-1}\right)+\omega^2\left(\tilde{\phi}_{k,1}-\tilde{\phi}_{k,-1}\right)\right]. \end{aligned} \quad (27)$$

3 Dispersion relation

The dispersion relation can be obtained by solving the following quasi-neutral equation group

$$\begin{aligned}&\tilde{n}_{\mathrm{i},k,m} = \tilde{n}_{\mathrm{ep},k,m} + \tilde{n}_{\mathrm{et},k,m}\ \ (m=\pm1),\\ &\tilde{n}_{\mathrm{i},k,0} - n_0(ka_{\mathrm{i}})^2 e\tilde{\phi}_{k,0}/T_{\mathrm{i}} = 0\ \ (m=0). \end{aligned} \quad (28)$$

Here, $a_{\mathrm{i}} \equiv (T_{\mathrm{i}}/m)^{\frac{1}{2}}/\omega_{\mathrm{i}}$ and the perturbed density for electrons is $\tilde{n}_{\mathrm{e}} = \sum_{l\neq0}(en_0/T_{\mathrm{e}})\tilde{\phi}_l\mathrm{e}^{\mathrm{i}l\theta}$ [11]. We add ions polarization density in quasi-neutral equation for $m = 0$. The reason is that for $m = 0$, ions' polarization density is large compared with electron's density $\tilde{n}_{\mathrm{e},k,0} = 0$, but for $m = \pm1$, ions' polarization density can be neglected compared with the electrons' perturbed densities $en_0\tilde{\phi}_{\mathrm{e},k,m}/T_{\mathrm{e}}$ due to the smallness of $k\rho_{\mathrm{i}}$. Substituting ions' and electrons' perturbed densities in Eqs. (4) and (27) into the quasi-neutral equations for $m = \pm1$ components, the expressions of $\tilde{\phi}_{k,\pm1}$ are derived

$$\tilde{\phi}_{k,\pm1} = \frac{\mp\left[\frac{\mathrm{i}k\omega qR}{2\omega_{\mathrm{i}}T_{\mathrm{i}}}\left(\frac{Z(\zeta_{\mathrm{i}})}{2\zeta_{\mathrm{i}}}+Z_1(\zeta_{\mathrm{i}})\right)-\frac{\sqrt{2}\bar{\omega}_{\mathrm{de}}\omega q^2R^2}{\mathrm{i}\pi^{1/2}\sqrt{\epsilon}T_{\mathrm{e}}v_{\mathrm{te}}^2}\left(1+\zeta_{\mathrm{e}}Z(\zeta_{\mathrm{e}})\right)\right]\tilde{\phi}_{k,0}}{\left(\frac{1}{T_{\mathrm{e}}}+\frac{(1+\zeta_{\mathrm{i}}Z(\zeta_{\mathrm{i}}))}{T_{\mathrm{i}}}+\frac{4\sqrt{2\epsilon}\zeta_{\mathrm{e}}^2}{\pi^{1/2}T_{\mathrm{e}}}\left(1+Z(\zeta_{\mathrm{e}})\zeta_{\mathrm{e}}\right)\right)}. \quad (29)$$

The governing equation is gained by substituting Eqs. (3) and (29) into the quasi-neutral equation of $m = 0$. After simplification, it becomes

$$\begin{aligned}&-\left(\frac{Z(\zeta_{\mathrm{i}})}{2\zeta_{\mathrm{i}}}+\frac{Z_1(\zeta_{\mathrm{i}})}{2}+Z_3(\zeta_{\mathrm{i}})\right)\\ &+\frac{\tau\zeta_{\mathrm{i}}^2\left(\frac{Z(\zeta_{\mathrm{i}})}{2\zeta_{\mathrm{i}}}+Z_1(\zeta_{\mathrm{i}})\right)^2}{1+\tau(1+\zeta_{\mathrm{i}}Z(\zeta_{\mathrm{i}}))+4\sqrt{2\epsilon}\pi^{-1/2}\zeta_{\mathrm{e}}^2(1+Z(\zeta_{\mathrm{e}})\zeta_{\mathrm{e}})}\\ &+\frac{\frac{\tau 2\sqrt{2\epsilon}m_{\mathrm{e}}\zeta_{\mathrm{e}}^2}{\pi^{1/2}m_{\mathrm{i}}}(1+\zeta_{\mathrm{e}}Z(\zeta_{\mathrm{e}}))\left(\frac{Z(\zeta_{\mathrm{i}})}{2\zeta_{\mathrm{i}}}+Z_1(\zeta_{\mathrm{i}})\right)}{1+\tau(1+\zeta_{\mathrm{i}}Z(\zeta_{\mathrm{i}}))+4\sqrt{2\epsilon}\pi^{-1/2}\zeta_{\mathrm{e}}^2(1+Z(\zeta_{\mathrm{e}})\zeta_{\mathrm{e}})}-\frac{1}{q^2}\\ &=0. \end{aligned} \quad (30)$$

The third term in the left hand of Eq. (30) originates from trapped electrons. We will directly solve Eq. (30) by numerical method to get the frequency and damping rate.

4 Numerical study

In this section, we will numerically solve Eq. (30) to get GAM's frequency and damping rate as functions of q and ϵ, respectively. To numerically solve the governing equation, the plasma dispersion function is transformed to

$$Z(\zeta) = e^{-\zeta^2}\left(\mathrm{i}\pi^{1/2} - 2\int_0^{\zeta}\mathrm{e}^{x^2}\mathrm{d}x\right). \quad (31)$$

With the assumption of thermal equilibrium between ions and electrons, the expressions $\tau = 1$ and $v_{\mathrm{te}}/v_{\mathrm{ti}} \approx 40$ hold. In this paper, ϵ is chosen to be in the range $[0.01, 0.4]$ to ensure $\bar{\omega}_{\mathrm{de}} \ll \omega_{\mathrm{be}}$.

4.1 The effect of q on GAM's dispersion

GAM's frequency and damping rate as functions of q are studied by specifying $\epsilon = 0.3$ and locating q in the range [1,7] as shown in Figs.1 and 2. GAM's frequency is a decreasing function of q as shown in Fig. 1, which is pointed out by Refs. [8,13]. Fig. 1 also reveals that the component of trapped electrons slightly reduces GAM's frequency in high q range.

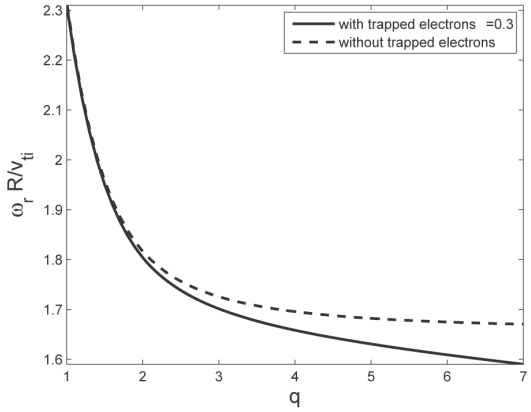

Fig.1 The comparison of GAM's frequency as a decrease function of q

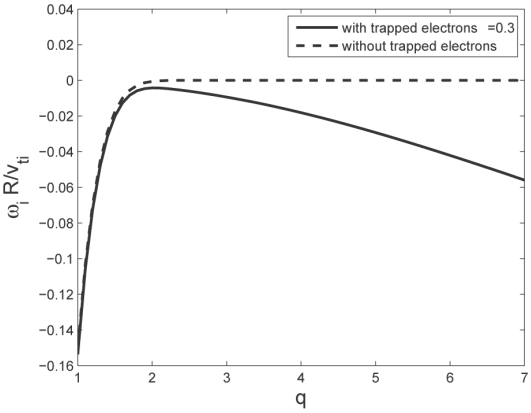

Fig.2 The comparison of GAM's damping rate as a function of q

The reason for slightly changing rate of GAM's frequency by electrons' trapped rate ϵ is revealed by Eq. (27). In Eq. (27), the non-adiabatic part of trapped electrons' perturbed density contributes to electrons' trapped effect on GAM's frequency. This perturbed density contains two parts. The first is proportional to $\sqrt{\epsilon}\bar{\omega}_{\rm de}\zeta_{\rm e}\tilde{\phi}_{k,0}/\omega_{\rm b}$. The second one is proportional to $\sqrt{\epsilon}\zeta_{\rm e}^2\tilde{\phi}_{k,1}$. In the considered regime, $\zeta_{\rm e} < 1$ and $\tilde{\phi}_{k,\pm1}/\tilde{\phi}_{k,0} \approx \bar{\omega}_{\rm de}/\omega_{\rm b}$ exist. Further, for $\zeta_{\rm e}$, $1 + \zeta_{\rm e}Z(\zeta_{\rm e})$ can be approximated as follows

$$1 + \zeta_{\rm e}Z\left(\zeta_{\rm e}\right) \approx 1 - 2\zeta_{\rm e}^2 + \frac{4}{3}\zeta_{\rm e}^4 - {\rm i}\zeta_{\rm e}{\rm e}^{-\zeta_{\rm e}^2}. \qquad (32)$$

So the trapped electrons' non-adiabatic effect (trapped effect) on GAM's frequency is $O(\zeta_{\rm e})$ order smaller compared with the adiabatic part on GAM's frequency. When ϵ becomes larger, $\zeta_{\rm e}$ becomes inversely smaller, GAM's frequency is less affected by large ϵ as shown in Fig. 4, which also shows that GAM's frequency is affected more obviously by small ϵ, consistent with our analysis.

The damping rate induced by circulating ions as shown in Fig. 2 decreases exponentially when q increases, because as q increases, $\zeta_{\rm ir}$, where r represents the real part, becomes larger. However, as a comparison, trapped-electrons-induced damping is an increasing function of q shown in Fig. 2, and as q increases, the amplitude of this damping rate becomes comparable to that induced by circulating ions in low q range.

The explanation for the increasing of trapped-electron-induced damping rate with q is as follows. To make Landau resonance happen, the equities $v_{\parallel}/v_{\rm ti} \approx \zeta_{\rm i}$ for circulating ions in Eq. (2) and $v/v_{\rm te} \approx \zeta_{\rm e}$ for trapped electrons in Eq. (25) should hold. When q increases, $\zeta_{\rm ir}$ becomes much larger than one, but $\zeta_{\rm er}$ is close to 1 as shown in Fig. 3, which implies that the circulating ions' resonant velocity becomes much larger than $v_{\rm ti}$, but the trapped electrons' resonant velocity is close to $v_{\rm te}$. So as q increases, the number of resonant circulating ions decreases, whiles the number of resonant trapped electrons increases.

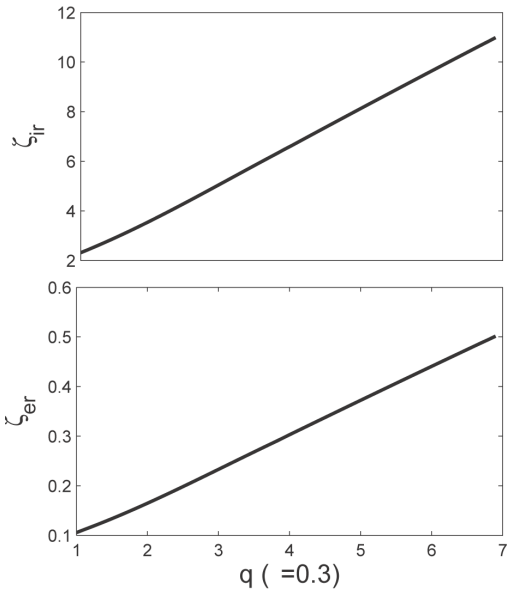

Fig.3 $\zeta_{\rm ir}$ and $\zeta_{\rm er}$ as a function of q with $\epsilon = 0.3$

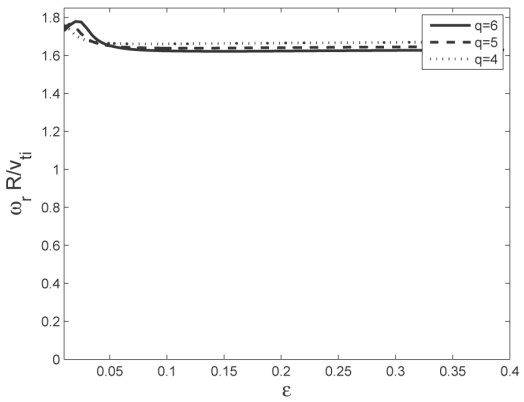

Fig.4 GAM's frequency as a function of ϵ for $q = 4$, 5, 6 with trapped electron effect included

4.2 The effect of ϵ on GAM's dispersion

The variations of GAM's frequency and damping rate as functions of ϵ are studied in Figs. 4-6, where parameter ϵ is chosen in $[0.01, 0.4]$ and q are specified by three values $4, 5, 6$, to observe the combined effect of ϵ and q on GAM's dispersion. Fig. 4 shows that trapped electrons has nearly no effect on GAM's frequency in the range $\epsilon \in [0.01, 0.4]$.

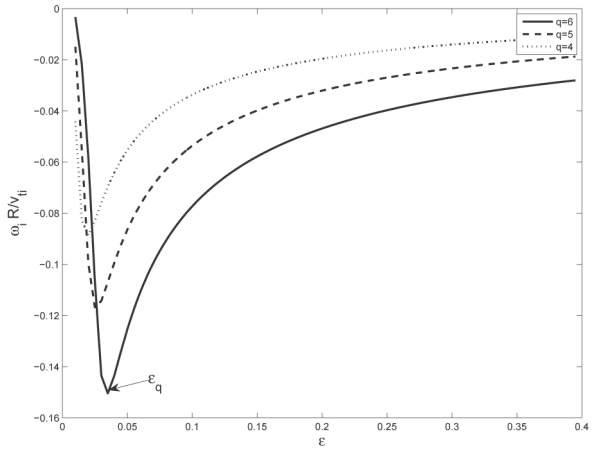

Fig.5 GAM's damping rate as a function of ϵ for different $q = 4, 5, 6$ with trapped electron effect included

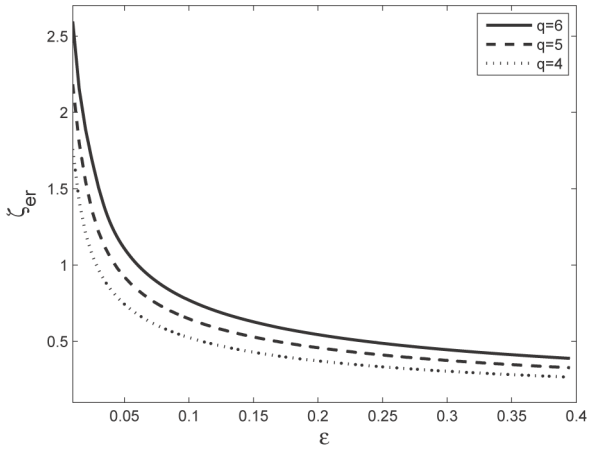

Fig.6 $\zeta_{\rm e}$ as a function of ϵ for different $q = 4, 5, 6$ with trapped electron effect included

As Fig. 5 shows, the amplitude of damping rate has a maximum value in the chosen ϵ range. For specified q, the maximum damping rate locates at a point where $\epsilon = \epsilon_q$. When $\epsilon < \epsilon_q$, damping rate decreases quickly to zero. And when $\epsilon > \epsilon_q$, damping rate decreases gradually. To explain this phenomena, it's needed to analyze Eq. (25) where trapped-electrons-induced damping comes from. According to Plemelj formula, the term $\zeta_{\rm e} Z(\zeta_{\rm e})$ in Eq. (25) can be reformulated as

$$\zeta_{\rm e} Z\left(\zeta_{\rm e}\right) = \int_{-\infty}^{+\infty} {\rm d}v \frac{\zeta_{\rm e} {\rm e}^{-v^2}}{v - \zeta_{\rm e}}$$

$$= -{\rm i}\pi\zeta_{\rm e}{\rm e}^{-\zeta_{\rm e}^2} + P\int_{-\infty}^{+\infty} {\rm d}v \frac{\zeta_{\rm e}{\rm e}^{-v^2}}{v - \zeta_{\rm e}}. \qquad (33)$$

When $\zeta_{\rm e} = 1$, the imaginary part in Eq. (33) reaches the maximum value, which implies that the largest damping rate reaches when trapped electrons' resonant velocity equals to electrons' thermal velocity. On the other hand, as shown by Fig. 6, $\zeta_{\rm er}$ approaches 1 as ϵ is close to ϵ_q. So it's understood that for specified q, when ϵ decreases to ϵ_q, the trapped electrons' resonant velocity is close to electrons' thermal velocity, where the density of trapped electrons distributed is much larger than that distributed in any other velocity range based on the assumption of Maxwellian distribution for electrons. However, when ϵ becomes smaller than ϵ_q, $\zeta_{\rm er}$ become larger than one just as shown in Fig. 6, which causes the damping rate decreases quickly to zero.

However, our formula can't stand for much smaller ϵ because $\bar{\omega}_{\rm de} > \omega_{\rm be}$ is required. As we have proved, trapped electrons effect on standard GAM's frequency can be ignored. So as ϵ becomes much smaller, $\omega_{\rm be} < \omega_{\rm de} < \omega_{\rm G}$ holds, which makes GAM's damping induced by trapped electrons can't happen. On the other hand, as ϵ decreases, the number of trapped ions becomes smaller, thus circulating-ion-induced damping will increase as pointed out in Ref. [19].

5 Summary and discussion

In this paper, we adopted drift kinetic theory for the study of collisionless damping on GAM. Besides resonance between circulating ions and GAM, trapped electron effect on damping is included. Electrostatic potentials of $m = 0, \pm 1$ are kept to study the modes coupling effect. To get trapped electrons perturbed distribution function, gyro orbit center reference frame is transformed to banana orbit center reference frame. The assumption of $\bar{\omega}_{\rm de}/\omega_{\rm be} \ll 1$ is adopted, so ϵ should not be very small and is chosen in $[0.01, 0.4]$. Resonance between ω and $\pm n\omega_{\rm b}$ is calculated only for $n = 1$. We found that trapped electrons nearly has no effect on GAM's frequency, but affect GAM's damping especially in the edge plasma in tokamaks. The reason for this damping effect is that the number of resonant trapped electrons become larger, since, as q increases, circulating ions' resonant velocity is far from $v_{\rm ti}$, but trapped electrons' is close to $v_{\rm te}$. Another result is that the amplitude of trapped-electrons-induced damping reaches a maximum value when $\epsilon = \epsilon_q$ for specified q. When ϵ varies from ϵ_q to zero, the amplitude decreases quickly to zero, and when $\epsilon > \epsilon_q$, the amplitude decreases gradually. Because when $\epsilon = \epsilon_q$, trapped electrons' resonant velocity equals electrons' thermal velocity, and in the range $\epsilon > \epsilon_q$ ($\epsilon < \epsilon_{\rm q}$), the resonant velocity is less (larger) than electrons' thermal velocity.

As shown in Fig. 2, when q reaches 7, which is at the plasma edge in tokamaks, trapped-electron-induced damping rate reaches a value comparable to that induced by circulating ions in the low q range. Such a high damping rate may explain the phenomena that GAM disappears whiles low frequency zonal flow

(LFZF) still exists during L-H transition in the edge plasma in tokamak, where temperature gradient and density gradient drive drift wave turbulence [5]. The nonlinear interaction of drift wave turbulence can provide energy for GAM [5] and LFZF. On the other hand, LFZF suffers collision damping, whiles GAM suffers collision and collisionless damping. The latter one is induced by circulating ions and trapped electrons. As shown in Refs. [8,13] and in Fig. 1, when q increases, damping rate induced by circulating ions decreases too fast to be counted in the edge plasma. Thus trapped electrons play an important role in collisionless damping at this range. During L-H transiton, GAM disappear while LFZF doesn't, which suggests that the collision damping rate enforced on GAM and LFZF may not be strong enough to damp GAM, that's to say that trapped-electron-induced damping plays a role in GAM'S disappearance in the edge plasma.

Acknowledgments

The authors would like to thank Professor Qin Hong, Dr. Huasen Zhang, Dr. Defeng Kong, and Dr. Lei Ye for their helpful discussions.

References

1 Winsor N, Johnson J L, Dawson J M. 1968, Phys. Fluids., 11: 2448
2 Melnikov A V, Vershkov V A, Eliseev L G, et al. 2006, Plasma Phys. Contr. F., 48: S87
3 Ido T, Miura Y, Kamiya K, et al. 2006, Plasma Phys. Contr. F., 48: S41
4 Fujisawa A. 2009. Nucl. Fusion, 49: 013001
5 Diamond P H, Itoh S I, Itoh K, et al. 2005, Plasma Phys. Contr. F., 47: R35
6 Xu M, Tynan G R, et al. 2012, Phys. Rev. Lett., 108: 245001
7 Miki K, Kishimoto Y, Miyato N, et al. 2008, J. Phys.: Conf. Ser., 123: 012028
8 Gao Z, Itoh K, Sanuki H, et al. 2006, Phys. Plasmas., 13: 100702
9 Zhang H S, Lin Z. 2010, Phys. Plasmas., 17: 072502
10 Hazeltine R D, Meiss J D. 2003, Plasma Confinement. Addison-Wesley Press
11 Gao Z, Itoh K, Sanuki H, et al. 2008, Phys. Plasmas., 15: 072511
12 Qiu Z, Zonca F, Chen L. 2010, Plasma Phys. Contr. F., 52: 095003
13 Sugama H, Watanabe T H. 2006, J. Plasma Phys., 72: 825
14 Wang L, Dong J Q, Shen Y, et al. 2011, Plasma Phys. Contr. F., 53: 095014
15 Chavdarovski I, Zonca F. 2009, Plasma Phys. Contr. F., 51: 115001
16 Tsai S, Chen L. 1993, Phys. Fluids B: Plasma Phys., 5: 3284
17 Zonca F, Chen L. 2000, Phys. Plasmas., 7: 4600
18 Rutherford P H, Frieman E A. 1968, Phys. Fluids., 11: 569
19 Gao Z. 2011, Plasma Sci. Technol., 13: 15

(Manuscript received 19 April 2013)
(Manuscript accepted 30 June 2013)
E-mail address of ZHANG Shuangxi:
shuangxi@mail.ustc.edu.cn